17. T. D. Butler, L. K. Cloutman, J. K. Dukowicz, and J. K. Ramshaw, Prog. Energy Combust. Sci., 7, 293-315 (1981).
18. P. O. Witze, Sandia Report N81-8242, Livermore (1981).
19. F. H. Harlow and A. A. Amsden, J. Comp. Phys., 8, 197-213 (1971).
20. W. Rivard, T. Butler, and O. Farmer, Numerical Solution of Problems in Hydromechanics [Russian translation], Moscow (1977).
21. S. Khert, Numerical Methods in Fluid Mechanics [in Russian], Moscow (1973), pp. 156-164.
22. B. D. Dali, Numerical Solution of Problems in Hydromechanics [in Russian], Moscow (1977), No. 14, pp. 143-156.
23. J. F. Thompson, F. C. Thames, and C. W. Mastin, J. Comput. Phys., 15, 299-319 (1974).
24. P. D. Thomas and J. F. Middlekoff, Raket. Tekh. Kosmonavt., 18, No. 7, 55-61 (1980).
25. N. N. Yanenko, N. T. Danaev, and D. V. Liseikin, Numerical Methods in the Mechanics of Continuous Media [in Russian], Novosibirsk (1977), Vol. 8, No. 4, pp. 157-163.
26. C. Arcoumanis, A. F. Bicen, and J. H. Whitelaw, Trans. ASME J. Fluids Eng., 105, 105-112 (1983).
27. C. Bassoli, G. Biaggini, G. Bodritti, and G. M. Cornetti, "Two-dimensional combustion chamber analysis of direct injection diesel," SAE Tech. Paper Ser. (1984).

STRUCTURE OF INHOMOGENEOUS MEDIA WITHIN THE RANDOM FRACTAL MODEL

R. R. Nigmatullin and N. N. Sutugin

UDC 536.7

The porosity of inhomogeneous media is treated within the random fractal model. Analytic expressions are obtained for the size distribution curves of bulk mesopores.

The concepts of a fractal and fractal dimensionality [1] are extremely fruitful in describing the geometry of heterogeneous systems, in the study of percolation effects, properties of various self-similar objects and structures, generated in hydrodynamics, astrophysics, electrochemistry, and other disciplines. More detailed information can be found, for example, in the reviews [2, 3]. The extension of the concept of a regular fractal and the introduction of a set of inhomogeneous objects with distributed values of fractal dimensionality became possible due to the multifractal approach, a topic discussed in the studies [4, 5].

Besides this extended class of regular fractals another is possible, which, as far as we are concerned, is a more natural method of introducing fractals, where the fractal scale, and not its dimensionality, occupies the role of the random fractal. The random fractal model (RFM) is proposed on the basis of the new concept of generalized fractal. The distribution function of various scales is found, and equations are obtained for the porosity of an inhomogeneous medium. The equations for two-phase system concentrations are generalized and interpreted if the distribution of one of the phases is fractal. A more detailed interpretation of experiments, related to measurements of porosity and the proof of their fractal occurrence in sandstones, is given within the RFM [6, 7]. Also analyzed was the size distribution function of bulk mesopores with the purpose of searching regions of fractal structure with its help. Comparison with experiment makes it possible to establish a number of new consequences and indicates internal consistencies of the model.

Description of Heterogeneous Media by Generalized Fractals. By means of some figure we divide the given volume V into original or elementary "volumes" $v_f(\Lambda) = G_f\Lambda^d$ with character-

V. I. Ul'yanov (Lenin) Kazan State University. Translated from Inzhenerno Fizicheskii Zhurnal, Vol. 57, No. 2, pp. 291-298, August, 1989. Original article submitted January 1, 1988.

 0022-0841/89/5702-0958$12.50

istic length Λ, which we define as the maximum scale of self-similarity. This implies that for scales $\eta \geq \Lambda$ the figure is assumed to be homogeneous, and its volume is determined by the expression $V = MG_f\Lambda^d$ (M is the number of elementary "volumes," and d is the Euclidean dimension, acquiring the integral values d = 1, 2, 3), and G_f is a geometric shape factor, taking into account the geometric shape of the figure selected as original cell. Thus, if the figure coincide with a segment of length Λ, then $G_f = 1$ (d = 1), for an equilateral triangular shape with edge Λ $G_f = \sqrt{3/4}$ (d = 2), for a tetrahedron $G_f = \sqrt{2/12}$, for a cube $G_f = 1$ (d = 3), etc.; for more complicated shapes G_f values can be found in [1]. The concept of $v_f(\Lambda)$ introduced above coincides with the definition of a physical elementary volume [8], and provides a lower boundary of the scale, starting with which the continuum approximation becomes valid.

We further partition the characteristic length Λ into k_1 parts, and select the scale $\eta_1 = \Lambda/k_1$. We fill the elementary volume by cells whose number equals p_1. Following the first partitioning phase, the volume is determined by the expression $v_1 = G_f p_1(\Lambda/k_1)^d$. For d = 3 and $p_1 = k_1^3$ we again obtain the original elementary volume, corresponding to its complete filling. Inhomogeneities occur only when $p_1 \neq k_1^3$. At the second phase we carry out a similar procedure in each of the p_1 cell formed again, selecting the scale $\eta_2 = \Lambda/k_1k_2$ and filling each of them by p_2 cells. Continuing the partitioning procedure, at the n-th phase we obtain the following equation for the volume of the elementary figure:

$$v_n = v_f(\eta_n) = p_n p_{n-1} \dots p_1 v_0(\eta_n) = G_f \frac{p_n p_{n-1} \dots p_1}{(k_n k_{n-1} \dots k_1)^d} \Lambda^d. \quad (1)$$

Introducing the notations $\tilde{p}^n = \prod_{j=1}^{n} p_j$, $\tilde{k}^n = \prod_{j=1}^{n} k_j$, expression (1) can be rewritten in the form

$$v_f(\tilde{\eta}) = G_f \tilde{\eta}^d (\Lambda/\tilde{\eta})^{\tilde{D}} = G_f \Lambda^{\tilde{D}} \tilde{\eta}^{d-\tilde{D}}. \quad (2)$$

Here $\tilde{\eta} = \Lambda/\tilde{k}^n$, $\tilde{D} = \ln \tilde{p}/\ln \tilde{k}$. If $p_i = p$, $k_i = k$ (i = 1, 2, ..., n), then expression (2) transforms to Eq. (3), determining the volume of a regular fractal [1]:

$$v_f(\eta) = G_f \eta^d (\Lambda/\eta)^D = G_f \Lambda^D \eta^{d-D} \quad (3)$$

with $\eta = \Lambda/k^n$, $D = \ln p/\ln k$. Even though expression (2) coincides in shape with (3), the dimensionality of $\tilde{D}$ and the effective scale $\tilde{\eta}$ have a different meaning than in (3). Expression (2) can be interpreted as the volume of the generalized fractal, determining the whole prehistory of partitioning, i.e., of the predominant structural memory. Unlike (2), the volume of the regular fractal (3) in all partitioning scales is an exact copy of the preceding partitioning, i.e., it possesses no self-similarity and structural memory. Therefore, it is fully justified to call the structure constructed by the method described above a generalized fractal, including a regular fractal and its combinations as special cases.

Random Fractal Model. The RFM promoted by us is based on three assumptions.

A-I. A heterogeneous medium can be described by a family of regular fractals, while the scale η is a continuous random quantity, whose variation limits are included in the interval (λ, Λ). The lower boundary of the interval λ determines the minimum possible scale (of the order of interatomic distances), starting with which a fractal can be formed. Let the probability of encountering scale η on the segment $[\eta, \eta + d\eta]$ be equal to $W(\eta)d\eta$; the mean volume is then determined by the expression

$$\langle v_f \rangle = \int_{\lambda}^{\Lambda} v_f(\eta) W(\eta) d\eta. \quad (4)$$

where $v_f(\eta)$ is given by Eq. (3). The second RFM assumption is introduced with the purpose of finding the shape of the function $W(\eta)$.

A-II. The set considered of regular fractals makes it possible to extract a dominating fractal with fractal dimensionality D, while the remaining fractals differ insignificantly from the dominant one in their parameters. Let p_i, k_i be the parameters of regular fractals, and let p and k be the parameters of the dominant fractal, while $p_i = p + \delta_i$, $k_i = k + \varepsilon_i$ (i = 1, 2, ..., n) and δ_i/p, $\varepsilon_i/k \ll 1$. In this case one can obtain the following expression from Eq. (2):

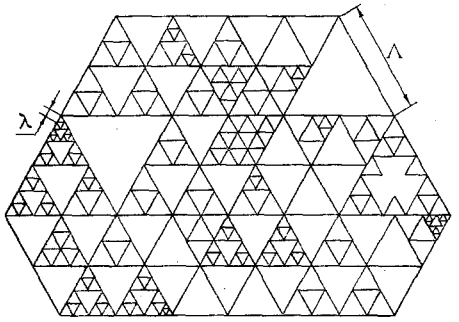

Fig. 1. A fractal structure consisting of Serpinskii structures; λ and Λ have dimensionality of length.

$$v_f(\eta) = G_f \eta^d \left(\frac{\Lambda}{\eta}\right)^{D+D'} \equiv G_f \Lambda^{D'} \eta^d \left(\frac{\Lambda}{\eta}\right)^{D} \eta^{\alpha}, \tag{5}$$

where D = ln p/ln k, and

$$-\alpha = D' = \frac{1}{\ln k}\left(\frac{\bar{\delta}}{p} - d\frac{\bar{\varepsilon}}{k} - \frac{\bar{\delta^2}}{2p^2} + d\frac{\bar{\varepsilon^2}}{2k^2} + \ldots\right). \tag{6}$$

In Eq. (6) $\bar{q}^s = n^{-1}\sum_{i=1}^{n} q_i^s$ ($q_i \equiv \delta_i,\ \varepsilon_i,\ s = 1,\ 2$) denotes the mean power arithmetic deviation ε_i, δ_i. It follows from expression (5) that the normalized scale distribution function W(η) is

$$W(\eta) = \frac{1+\alpha}{\Lambda^{1+\alpha} - \lambda^{1+\alpha}}\eta^{\alpha}. \tag{7}$$

As follows from (6), by its meaning the parameter α implies possible structural distortions of the dominant fractal. After substituting (7) into (3) and (4) we obtain the following expression for $\langle v_f \rangle$:

$$\langle v_f \rangle = G_f \frac{1+\alpha}{1+\alpha+d-D}\Lambda^d \frac{1-\mu^{1+\alpha+d-D}}{1-\mu^{1+\alpha}}. \tag{8}$$

Here μ denotes the ratio λ/Λ. Usually the self-similarity region occupies a large fraction of the scales, and therefore $\mu \ll 1$. As a result of the integration performed, under certain conditions a self-similar structure can be formed again, combining the various elements of regular fractals and possessing self-similarity in the average statistical sense. Therefore, it is advisable to request that the self-similar nature of the structure be retained. This requirement is also the Principle of Statistical Self-Similarity (PSSS) promoted by us, which is also the third assumption underlying the RFM. The mathematical expression of the PSSS is

$$\langle v_f \rangle = \tilde{G}_f \Lambda^{\bar{D}} \lambda^{d-\bar{D}} = \int_{\lambda}^{\Lambda} v_f(\eta) W(\eta)\, d\eta. \tag{9}$$

The results of investigating expression (9) with the purpose of clarifying the region of admissible α and μ values for which the PSSS is satisfied are shown in Table 1, where the notation D = d + 1 + α was introduced. It is seen from the table that only in the first two cases is the self-similar fractal nature of the structure retained. In case 3 the system of scales of order Λ becomes homogeneous. Due to the occurrence of a factor of type $\ln \mu^{-1}$ for cases 4 and 5, the PSSS is, strictly speaking, not satisfied, while in case 6 the obvious inequality D < d is not satisfied. In case 1 the dimensionality of the regular fractal D is an invariant quantity, while in case 2 the role of dimensionality is taken by the quantity $\bar{D} = d - |1 + \alpha|$, which we define as the dimensionality of the statistical fractal. Thus, the PSSS is satisfied only when the admissible α values are in the interval $-4 < \alpha < -1$, since $0 < D,\ \bar{D} < 3$.

An example of a random fractal is shown in Fig. 1, where the dominant fractal is selected to be a Serpinskii filling. Integration over all possible scale values in the interval (λ, Λ) leads to a statistically self-similar structure, having dimensionality D or $\bar{D}$, depending on whether case 1 or 2 is realized. The replacement of D by $\bar{D}$ implies that in the orig-

TABLE 1. Investigation of the Region of Admissible α Values

No.	Inequality concerning α	Inequality concerning $\mu = \lambda/\Lambda$	$\langle v_f \rangle$	$\tilde{G}_f$
1	$1+\alpha<0$, $1+\alpha+d-D<0$	$\mu^{\bar{D}-d}>1$, $\mu^{\bar{D}-D}\gg 1$	$\tilde{G}_f\Lambda^d\mu^{d-D}$	$G_f\frac{d-\bar{D}}{D-\bar{D}}$
2	$1+\alpha<0$, $1+\alpha+d-D>0$	$\mu^{\bar{D}-d}\gg 1$, $\mu^{\bar{D}-D}\ll 1$	$\tilde{G}_f\Lambda^d\mu^{d-D}$	$G_f\frac{d-\bar{D}}{\bar{D}-D}$
3	$1+\alpha>0$, $1+\alpha+d-D>0$	$\mu^{\bar{D}-d}\ll 1$, $\mu^{\bar{D}-D}\ll 1$	$\tilde{G}_f\Lambda^d$	$G_f\frac{\bar{D}-d}{\bar{D}-D}$
4	$1+\alpha<0$, $D=\bar{D}=d-(1+\alpha)$	$\mu^{\bar{D}-d}\gg 1$	$\tilde{G}_f \ln(\mu^{-1})\,\Lambda^d\mu^{d-D}$	$G_f(d-D)$
5	$1+\alpha=0$, $d-D>0$	$\mu^{d-D}\ll 1$	$\tilde{G}_f(\ln\mu^{-1})^{-1}\Lambda^d$	$G_f(d-D)^{-1}$
6	$1+\alpha>0$, $1+\alpha+d-D<0$	—	—	—

inal setting those fractals are widely represented, whose dimensionality exceeds insignificantly that of the dominant fractal ($\bar{D} - D > 0$), while in the opposite case ($\bar{D} - D < 0$) D is an invariant quantity. With account of the definition of $\bar{D}$, Eq. (9) can be rewritten in the form

$$\langle v_f \rangle = G_f \frac{\bar{D}-d}{\bar{D}-D}\Lambda^d \frac{1-\mu^{\bar{D}-D}}{1-\mu^{\bar{D}-d}}, \tag{10}$$

more convenient for determination of the porosity, as considered below. It is also noted that the insignificant deviations of the quantities k_i, p_i from k, p are accounted for by the parameters $\tilde{G}_f$ and α. The relation $\eta = \Lambda/k^n$ shows that the random scale variation can occur due to variations in k and n. The PSSS assumes that the random variation in η is primarily due to the random choice of the number of partition stages n of some elementary volume, having initial size Λ. The insignificant variations in k in terms of $\bar{\varepsilon}$, $\bar{\varepsilon}^2$, occurring in α [Ea. 6)], fix the structural inhomogeneities, assumed to be given.

Porosity. Comparison with Experimental Data. The porosity is defined as the ratio of the total volume of porous space V_p to the total volume of the sample V, bearing in mind the absolute porosity [6]. It is assumed that the pores in the medium form some fractal structure. To calculate the porosity

$$m = \frac{V_p}{V} \tag{11}$$

it is necessary to calculate the total volume of pores V_p. According to the discussion above, within the assumed RMF we have

$$V_p = M\langle v_f \rangle. \tag{12}$$

Here $\langle v_f \rangle$ is the mean volume of the statistical fractal, determined by Eq. (8) or (10), and $M = V/v_f(\Lambda)$, as earlier, is the number of statistical fractals at scales $\eta \sim \Lambda$, included in the whole volume of the body. Substituting Eqs. (12) and (10) into (11) leads to an expression for the absolute porosity in the form (d = 3):

$$m = \frac{\bar{D}-3}{\bar{D}-D}\,\frac{1-\mu^{\bar{D}-D}}{1-\mu^{\bar{D}-3}}. \tag{13}$$

In case 1 ($\bar{D} < D$) we have the following approximation from the exact expression (13)

$$m \simeq \frac{3-\bar{D}}{D-\bar{D}}\mu^{3-D}(1-\mu^{D-\bar{D}}+\ldots). \tag{14}$$

For case 2 ($\bar{D} > D$)

$$m \simeq \frac{3-\bar{D}}{\bar{D}-D}\mu^{3-\bar{D}}(1-\mu^{\bar{D}-D}+\ldots). \tag{15}$$

TABLE 2. Analysis of the Experimental Data of [7]

Sample	$\frac{D}{\overline{D}}$	$\frac{\overline{D}}{D}$	$\mu_{изм}$	$m_{изм}$	A	$m_{кт}$	m
TGS#965	$\frac{2,57}{0,04}$	$\frac{2,57}{2,216}$	$8\cdot10^{-4}$	5,45	1,170	4,68	5,3
TGS#466	$\frac{2,68}{\overline{D}<0}$	$\frac{2,68}{2,33}$	$3,3\cdot10^{-4}$	7,25	0,9428	7,645	7,3
Coconino	$\frac{2,78}{1,95}$	$\frac{2,78}{2,62}$	$2,04\cdot10^{-5}$	11,75	1,2645	9,645	11,0
Navajo	$\frac{2,81}{1,268}$	$\frac{2,81}{2,65}$	$4\cdot10^{-5}$	16,4	1,1232	14,8	15,7
St. Peter's	$\frac{2,87}{\overline{D}<0}$	$\frac{2,87}{2,74}$	$4\cdot10^{-5}$	26,0	0,970	26,905	26,4

Note. The porosity is given in percents.

Data are given in [7] of two experiments, used by us to verify expressions (13), (14). The reason for selecting [7] is that the results in it are those of two independent experiments, allowing one to reduce the number of free model parameters to a minimum. Firstly, by using techniques of electron scanning microscopy it has been established that a space of the order of Arizona sand grains (see Table 2) is fractal with a completely determined numerical value of the fractal dimensionality. Secondly, the Boyle method was used to measure the absolute sample porosity m_{meas}. Accurately within terms $\sim\mu|\overline{D} - D|$, Eqs. (14) and (15) coincide with the expression for the porosity, used by the authors of [7] for comparison with experimental data:

$$m = A\mu^{3-D}. \tag{16}$$

In this case it has been assumed that A = 1, and, consequently, the statistical nature of the structure of grain sands is unaccounted for. Equation (16) can be obtained from (3) (for $\eta = \lambda$) and definition (11). It is natural to compare the data provided in [7] with the RFM consequences, where, as follows from (14) and (15), the coefficient A differs from unity:

$$A = \pm\frac{3-\overline{D}}{D-\overline{D}},$$

where the plus sign refers to Eq. (14), and the minus sign – to (15). From the experimental data it is unclear what is the dimensionality measured by the authors of [7], D or $\overline{D}$, and therefore we started from two cases. In the first case $D > \overline{D}$, so that from the known value of $D = D_{meas}$ and the experimentally measured m_{meas} and μ_{meas} we calculated the coefficient A (column 6 of Table 2), and then the dimensionality $\overline{D}$ was found by Eq. (14). In the second case $\overline{D} > D$; here, from the measured values of $\overline{D} = D_{meas}$, m_{meas}, μ_{meas} we found the dimensionality D from Eq. (15). The calculation results are shown in Table 2. In the penultimate column we show for comparison results of calculations by Eq. (16) for A = 1. In the last column of the table the porosity was calculated by using the data obtained from D and $\overline{D}$ by the exact equation (13) with the purpose of verifying the accuracy of the approximate equations (14) and (15). The analysis carried out by us shows that for all five samples the authors of [7] measured the statistical fractal dimensionality, coinciding with D_{meas}. The values of the calculated dimensionality D are given in the third column. The assumption that $D = D_{meas}$ leads to meaningless results. Thus, the model suggested is substantially correct in interpreting the experimental data.

It must be noted that Eq. (13) makes it possible to deepen and broaden the concept of concentration in two-phase systems. The meaning of this concept becomes obvious if the structure of one of the phases is formed by clusters with scales in the interval (λ, Λ), and the arrangement of clusters in the sample has a fractally statistical nature. Indeed, if the porous space is filled by a differential material, the concentration of this phase with respect to the total volume is determined by an equation similar to (13), where the parameter μ determines the admitted region of fractality of the separated phase. Denoting by $V_i = M_i\langle v_f\rangle_i$ the volume of the i-th component, the relative content of the fractal component is determined by the equation

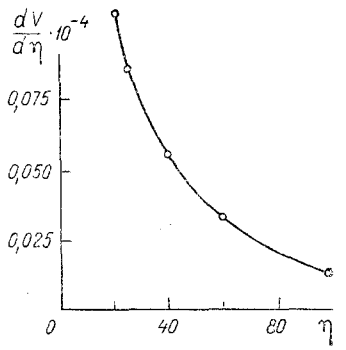

Fig. 2. Pore volume distribution function over sizes for betonite ([9], Fig. 60). $dV/d\eta$, cm^2; η, Å.

$$c_i = G_{fi}\Lambda^d \frac{M_i}{V} \frac{\overline{D}_i - d}{\overline{D}_i - D_i} \frac{1-\mu^{\overline{D}_i - D_i}}{1-\mu^{\overline{D}_i - d}}. \qquad (17)$$

Here D_i, $\overline{D}_i$ are the fractal dimensionalities of the i-th component. In our opinion, this equation is of large practical value in the study of multiphase systems of fractal nature.

Pore Volume Distribution Function over Sizes. The pore volume distribution function over sizes can be constructed by various experimental methods for porous systems. A typical curve of this type is shown in Fig. 2. For most materials the extremum of the curve is in a region of the order of tens of angstroms. It is natural to assume that the region of the curve on the side of large scale values can have a fractal nature. With the purpose of verifying this assumption we initially obtained the function $dv\eta/d\eta$ following from the RFM. Indeed, the probability of encountering a fractal of scale η in the interval $[\eta, \eta + d\eta]$ equals $dV(\eta) = v_f(\eta)W(\eta)d\eta$, where $v_f(\eta)$ and $W(\eta)$ are determined by Eqs. (3) and (7), respectively. Consequently, the pore volume distribution function over sizes is found by the expression

$$\frac{dV(\eta)}{d\eta} = G_f \Lambda^{d-\overline{D}+D} \frac{d-\overline{D}}{\mu^{\overline{D}-D}-1} \eta^{\overline{D}-D-1} \equiv B\eta^{\overline{D}-D-1}.$$

The constant B cannot be determined from experimental data, but the exponent $\overline{D} - D - 1$ can be calculated by representing the measured values in logarithmic coordinates. Thus, for the curve selected from [9] and shown in Fig. 2, we obtained $\overline{D} - D = -0.273$. The analysis of similar curves for a number of other materials, not provided due to lack of space, also displays fractal behavior, which is further verification of RFM principles.

Thus, the RFM suggested and the function $W(\eta)$ have been verified experimentally. The conclusions following from the model make it possible to expand on the nature of porosity, particularly on its fractal nature. As follows from Table 2, from the statistical fractal dimensionality $\overline{D}$ one can establish the dimensionality of the regular fractal D, and in turn construct the model of a porous system.

We would like to note the following practical aspects following from the RFM. Equations (9), (13), and (17) make it possible to deepen and expand the concepts of concentration and porosity, relating the structure of inhomogeneity to its possible fractal manifestation. This allows, in turn, more detailed treatment in important practical problems, such as determination oil-gas-saturation of collectors, explanation of the structure of alloys and solid solutions, the study of crystal growth features, etc. Experiments similar to [7] allow more detailed RFM verification as well as further improvement.

NOTATION

η, fractal scale; λ, Λ, minimum and maximum self-similarity fractal scales; μ, ratio of minimum to maximum self-similarity fractal scales; G_f, $\overline{G}_f$, geometric shape factors; D, $\overline{D}$, fractal dimensionalities of the regular and statistical fractals; $W(\eta)$, scale distribution function; α, parameter of the scale distribution function; $v_f(\eta)$, volume of a regular fractal of given scale η; $\langle v_f \rangle$, volume of a statistical fractal; V, sample volume; V_p, volume of empty space; M, number of volumes $v_f(\Lambda)$ in volume V; m, porosity; c_i, concentration of the i-th phase.

LITERATURE CITED

1. B. B. Mandelbrot, Fractal Geometry of Nature, Freeman, San Francisco (1982).
2. Ya. B. Zel'dovich and D. D. Sokolov, Usp. Fiz. Nauk, 146, 492-506 (1985).
3. I. M. Sokolov, Usp. Fiz. Nauk, 150, 221-225 (1986).
4. T. C. Halsey, M. Jensen, L. Kadanoff, et al., Phys. Rev., A33, 1141-1153 (1986).
5. L. Pietronero and A. P. Siebesma, Phys. Rev. Lett., 57, 1098-1101 (1986).
6. A. A. Khanin, Petrophysics of Oil and Gas Layers [in Russian], Moscow (1976).
7. A. J. Katz and A. H. Thompson, Phys. Rev. Lett., 54, 1325-1328 (1985).
8. L. I. Kheifets and A. V. Neimark, Multiphase Processes in Porous Media [in Russian], Moscow (1982).
9. F. D. Ovcharenko, Hydrophilic Nature of Clays and Clay Minerals [in Russian], Kiev (1961).

THERMAL CONDUCTIVITY OF HEPTYL CAPROATE AT HIGH TEMPERATURES AND PRESSURES

R. A. Mustafaev and M. A. Guseinov

UDC 536.6

Measurements have been made on the thermal conductivity of heptyl caproate at 305-611 K and 0.098-98 MPa.

Caproates are widely used in making aromatic additives for the food and perfumery industries as well as in food chemistry, but no systematic measurements have been made on their thermophysical parameters, although values are required to design optimized techniques.

Very few data have been published on caproate conductivities. Measurements have been made at Kazan' Technological Institute [1] on the temperature dependence at atmospheric pressure for the first two members of the homologous series. Heptyl caproate has not been examined before at all.

We have made measurements on caproates over wide temperature and pressure ranges [2] by dynamic monotone heating. The theory, the measurement methods, and the instruments have been described in [3]. Here we report results for heptyl caproate at 305-611 K and 0.098-98 MPa.

TABLE 1. Measured Conductivities $\lambda \cdot 10^3$ W/m·K for Hetpyl Caproate at Various Temperatures and Pressures

T, K	P, MPa						T, K	P, MPa					
	0,098	19,6	39,2	58,8	78,4	98		0,098	19,6	39,2	58,8	78,4	98
305	138	145	152	157	162	166	464	101	112	121	129	135	141
317	135	143	149	155	160	164	476	98,1	110	119	127	133	140
330	132	140	146	152	157	162	489	96,4	107	118	124	132	138
342	129	137	144	149	154	160	501	94,6	105	115	123	130	135
354	126	135	142	148	152	158	514		104	114	122	127	134
366	124	132	140	146	151	156	526		102	112	120	126	133
378	121	131	139	145	150	154	538		100	111	119	125	131
390	119	128	137	143	148	153	550		98,7	110	118	123	130
402	116	125	133	140	146	150	563		97,8	108	117	122	129
414	113	123	131	138	144	149	575		95,9	107	116	122	127
427	110	120	128	136	142	147	587		95,3	106	115	121	126
440	107	117	127	133	139	146	598		94,7	105	114	120	125
452	104	115	124	131	137	143	611		94,1	104	113	119	124

Il'drym Azerbaidzhan Polytechnical Institute, Baku. Translated from Inzhenerno-Fizicheskii Zhurnal, Vol. 57, No. 2, pp. 299-300, August, 1989. Original article submitted August 2, 1988.

 0022-0841/89/5702-0964$12.50